Supplemental Information

MATERIALS and METHODS

Metabolic work-up

The metabolic work-up included a detailed questionnaire and a clinical examination with anthropometry. All anthropometric measurements were performed in the morning, with patients in fasting conditions and undressed. Height was measured to the nearest 0.5 cm and body weight was measured with a digital scale to the nearest 0.2 kg. BMI was calculated as mass (in kilograms) over height (in meter) squared. Waist circumference was measured at the mid-level between the lower rib margin and the iliac crest. Hip circumference was measured at the level of the trochanter major. WHR was calculated by dividing waist circumference by hip circumference. Body composition was determined by bio-impedance analysis as described by Lukaski et al. (1), and fat mass (%) was calculated, using the formula of Deurenberg et al. (2). The cross-sectional areas of total abdominal adipose tissue (TAT), VAT and subcutaneous abdominal adipose tissue (SAT) were measured by CT at L4-L5 level according to previously described methods (3). Systolic and diastolic blood pressure were determined on the right arm of the patient, after at least 5 min rest, using a mercury sphygmomanometer.

A fasting blood analysis (taken from an antecubital vein) included blood cell count, coagulation tests, electrolytes and kidney function tests, lipid profile [total cholesterol, high-density lipoprotein cholesterol (HDL-C), and triglycerides (TG)], liver tests [aspartate aminotransferase (AST), alanine aminotransferase (ALT), lactate dehydrogenase (LDH), gamma glutamyl transpeptidase (GGT), alkaline phosphatase (ALP), total bilirubin and fractions], high-sensitive C-reactive protein (hs-CRP), creatinine kinase, total protein, protein electrophoresis, thyroid function, ferritin, vitamin B12, folic acid. Low-density lipoprotein cholesterol (LDL-C) was calculated using the Friedewald formula (4).

A 3-h oral glucose tolerance test (OGTT) with 75g of glucose with sampling at 0, 15, 30, 60, 90, 120, 150 and 180 minutes was carried out, insulin and C-peptide were also determined at 0, 30, 60, 120 and 180 minutes. Insulin resistance was estimated using homeostasis model assessment (HOMA-IR) as described by Matthews et al. (5), and was calculated as [insulin (mU/L) x glucose (mmol/L)]/22.5, with 1 as reference value for normal insulin sensitivity. Area under the curve (AUC) for glucose and insulin was calculated using all 8 sampling points (for glucose) and all 5 sampling points (for insulin and C-peptide) using the trapezoid method. Glucose tolerance status was defined based on the criteria of the American Diabetes Association (6). Metabolic syndrome was defined following the harmonized definition by Alberti et al. (7).

Plasma glucose, total cholesterol and TG were measured on Vitros 750 XRC (Ortho Clinical Diagnostics, Johnson & Johnson, UK). HDL-C was measured on Hitachi 912 (Roche Diagnostics, Germany). Insulin levels were measured with the Medgenic two-site IRMA assay (BioSource, Belgium). C-peptide was determined by electrochemiluminescence immunoassay (ECLIA) on'Modular E170 (Roche, Switzerland). Hs-CRP was assayed with nephelometry on BNII (Siemens Healthcare Diagnostics, Brussels, Belgium). AST, ALT, and γGT were measured by "photometry" on Dimension Vista® 1500 System (Siemens, USA).

Hepatological work-up: The liver specific program included additional blood analysis to exclude the classical etiologies of liver disease (for example, viral hepatitis and autoimmune disease) [s-choline-esterase, carcino-embryonic antigen, α-fetoprotein, anti-nuclear factor, anti-neutrophil cytoplasm antigen antibodies, anti-smooth muscle antibodies, anti-mitochondrial antibodies, anti-liver–kidney microsome antibodies, serum copper and coeruloplasmin, α-1-antitrypsin, anti-Hepatitis B core antibodies, anti-Hepatitis B surface antigen, anti-Hepatitis C virus antibodies], a Doppler ultrasound of the abdomen with parameters of liver and spleen volume and liver vascularization, a liver–spleen scintigraphy using technetium-99m (99mTC) tin colloid (8) and an aminopyrine breath test as a measure for liver metabolic reserve (9). Patients were excluded from further analysis if another liver disease was diagnosed.

In a sub cohort of patients some additional laboratory tests were performed. Cytokeratin 18 (CK-18), a promising serum marker of liver fibrosis, was determined, in collaboration with Bram Blomme (University of Ghent), using a two-enzyme-linked immunosorbent assay (PEVIVA AB, Bromma, Sweden) according to the manufacturer's instructions (10). The rs738409 polymorphism (c.444C>G, encoding pI148M) of patatin-like phospholipase domain-containing protein 3 (PNPLA3) was analyzed as described previously (11).

FIGURE and TABLE LEGENDS

Supplemental Figures:

Supplemental Figure 1 – Global analysis of varying transcripts in liver from human NASH patients. A) Self organizing map of transcripts. RNAs were analyzed on Affymetrix gene chips (HuGene ST2.0) and data processed using the Genespring v13.1 software as described in the Material and methods section. After quantile normalization, raw data were filtered to exclude the lowest expressed transcripts (5%

percentile). Non coding RNAs (lncRNAs and miRNAs) were also excluded from further analysis to select only mRNAs coding for proteins (6,925 entities). Gene-level normalized intensities were generated and data complexity was reduced by building a self-organizing map using a squared Euclidian distance metrics with 1,500 iterations allowing 10 gene clusters to be defined. Red indicates expression over the median, green indicates expression below the median. B) Gene Ontology (GO) term enrichment of identified clusters. Gene lists corresponding to each cluster were uploaded in the David functional annotation tool. Enriched biological terms were identified against the indicated databases (OMIM, PIR, GO, Biocarta and Kegg databases). The top hit for each database is indicated along with the number of genes belonging to the identified biological term (gene count), the enrichment ratio (%), the p value (p value) and the corrected p value [(by the Benjamini-Hochberg false discovery rate procedure, p value (BH)].

Supplemental figure 2 - General strategy for the analysis of human liver transcriptomes. Following a standardized analysis procedure, microarray data from our study were processed to generate a gene list showing varying expression in at least one condition. The cohort was classified according to the indicated clinical, biochemical and histological parameters to identify genes associated to disease progression. A meta-analysis was carried out using 2 publicly available datasets and genes common to the 3 studies generated a human core signature for advanced NASH.

Supplemental figure 3 - Differential gene expression in human fibrotic livers. A) Volcano plot of differentially expressed genes in fibrotic livers. Gene expression levels were compared between non fibrotic (F0) and fibrotic (F2-4) livers. The threshold for significant differential expression was set at a fold change of 1.2, with a p value of 0.05. Blue: significantly down-regulated genes, red: significantly up-regulated genes. Lists of genes in these 2 categories can be found in Supplemental Table 2. B) Gene ontology term enrichment of significantly down- (blue) or up-regulated (red) genes in fibrosis. Gene lists of differentially expressed genes were searched against the Biological Process function annotation table of Metascape (settings: minimum overlap 5, p value cutoff 0.01, minimum enrichment 5). Statistically enriched terms were converted into a network layout in which circle diameters are proportional to the number of genes and the thickness of edges indicates the similarity score. Inset: The color scale indicates the p value of the nodes.

Supplemental figure 4 - Detailed GO term enrichment of genes normalized by GBP. A GO term enrichment against the BP FAT was performed as in Figure 1C. The complete listing of enriched terms is shown. Inset: p value of the nodes. A complete list of genes can be found in supplemental table 6.

Supplemental figure 5 - Multi-gene list enrichment analysis for biological themes in NASH+fibrosis patients. Gene lists corresponding to up-regulated genes in each mentioned study were analyzed to identify terms that are statistically enriched in the Biological Process (BP) function annotation table. Common themes were identified and visualized as a network plot. Each node is a pie chart representing the proportion of genes from each gene list under the indicated, most significant BP annotation. The size of the node is proportional to the number of genes within that node. A complete gene list is available in supplemental Table 7.

Supplemental figure 6 – Defining a human gene signature for NASH+fibrosis. Differentially expressed genes in NASH+fibrosis patients were identified as described in the Material and Methods section using the indicated datasets. Circos plots of up-(A) or down-(B) regulated genes were generated using Metascape and gene symbols shared by all 3 studies are indicated below. Yellow: indicates GBP-sensitive genes.

Supplemental Figure 7 - Hepatic gene regulation in MCD/HF diet-fed mice. Differentially expressed genes in chow diet-fed mice vs. MCD/HF diet-fed mice were identified as described in the Material and Methods section. Genes displaying a FoldChange > 5, $p<0.05$ (unpaired t-test, Benjamini-Hochberg post-hoc test) were identified and up- (A) or down-regulated (B) gene lists underwent a GO term enrichment against the Biological Process function annotation table (Metascape, settings: minimum overlap 5, p value cutoff 0.01, minimum enrichment 5). Statistically enriched terms were converted into a network layout in which circle diameters are proportional to the number of genes and the thickness of edges indicates the similarity score. Inset: The color scale indicates the p value of the nodes. A complete list of genes can be found in Supplemental Table 8.

Supplemental Figure 8 - Hepatic gene regulation in CCl_4-treated, HF diet-fed mice. Differentially expressed genes in chow diet-fed mice vs. CCl_4-treated, HF diet-fed mice were identified as described in the Material and Methods section. Genes displaying a FoldChange > 5, $p<0.05$ (unpaired t-test, Benjamini-Hochberg post-hoc test) were identified and up- (A) or down-regulated (B) gene lists underwent a GO term enrichment against the Biological Process function annotation table (Metascape, settings: minimum overlap 5, p value cutoff 0.01, minimum enrichment 5). Statistically enriched terms were converted into a network layout in which circle diameters are proportional to the number of genes and the thickness of edges indicates the similarity score. Inset: The color scale indicates the p value of the nodes. A complete list of genes can be found in supplemental table 9.

Supplemental figure 9 – *DPT* expression correlates with the fibrosis stage. DPT expression was assayed by RT-qPCR and after normalization to *36B4* content, results were expressed as the mean +/- SEM (n=6-35) relative to control (NAS score=0, A or Fibrosis stage=0, B). Data were compared using a two-tailed ANOVA corrected for multiple comparisons using the Dunnett's post hoc test. *, $p<0.05$, **, $p<0.01$, ***, $p<0.005$. Please note that data shown in panel B are also shown in Figure 3A.

Supplemental figure 10 – SMAD3 protein and phosphorylation levels. Whole liver extracts were analyzed on a Wes capillary electrophoresis device (ProteinSimple) and the content in SMAD3 and in phospho-SMAD3 were measured using specific antibodies (XXXX) as recommended by the manufacturer.

Supplemental figure 11 – miRNA expression in liver. *miR21* and *miR122* expression levels were assayed by RT-QPCR using Taqman probes and normalized to sno234 expression. Results were expressed as the mean +/- SEM (n=6-8) relative to control (Dpt+/+, untreated). Data were compared using a two-tailed ANOVA corrected for multiple comparisons using the Dunnett's post hoc test. *, $p<0.05$, **, $p<0.01$, ***, $p<0.005$.

Supplemental Figure 12 – Hepatic PPARα expression in AAV8-TBG-PPARα transduced mice. Mice were injected with PPARα-encoding AAV8 viral particles and the expression of wild type or mutated PPARα was monitored by western blot analysis of liver lysates 2 weeks after injection. The 2 western blots are derived from different gels.

Supplemental Tables:

Supplemental table 1 – SOM clustering of regulated liver genes. RNAs were analyzed on Affymetrix gene chips (HuGene ST2.0) and data processed using the Genespring v14.3 software as described in the Material and methods section. After quantile normalization, raw data were filtered to exclude the lowest expressed transcripts (5%percentile). Non coding RNAs (lncRNAs and miRNAs) were also excluded from further analysis to select only mRNAs coding for proteins (6,925 entities). An Excel file containing the 6,925 genes organized into 10 clusters after SOM processing is provided (Gene symbols and SOM clusters worksheet). Associated keywords are also shown in Supplemental Figure 1 (KW association worksheet).

Supplemental Table 2 – Cohort stratification, gene expression patterns and GO term enrichment analysis. Normalized gene expression values were used to identify genes displaying varying expression as a function of biometric, biochemical or histological parameters. Genes that were either up- (X-up) or down-regulated (X-down) (FC>1.2, p<0.05) are indicated (genesymbol column) and top hits from GO term enrichment analysis are shown, along with the number of genes tagged with this term (gene count), the percentage of genes from the list tagged with this term (%), p-value and corrected p-value.

Supplemental Table 3 – Regulated genes in NASH or fibrosis. Data were extracted from supplemental table 2 to generate a list of 193 up-regulated genes in NASH (lobular inflammation and ballooning) or in fibrosis. A similar approach was applied to generate a list of 58 down-regulated genes.

Supplemental Table 4 – Effect of bariatric surgery on lobular inflammation-associated genes. Gene expression values from patients who underwent bariatric surgery and displayed a significant reduction in the lobular inflammation score 1 year after intervention (M12, with a score ≥2) were compared to those at baseline (M0, see also Supp. Figure 3). Data complexity was reduced by building a self-organizing map using a squared Euclidian distance metrics with 1,500 iterations allowing 10 gene clusters to be defined. These clusters are shown and those containing significantly dysregulated genes (paired t-test, FC>1.2, p<0.05; clusters 1-2 and 9-10) were annotated by GO term enrichment analysis (Supp. Figure 3) and selected for further analysis. Gene symbols are indicated below each cluster diagram which was generated using Genespring GX14.3.

Supplemental Table 5 – Effect of bariatric surgery on fibrosis-associated genes. Gene expression values from patients who underwent bariatric surgery and displayed a significant reduction in the fibrosis score 1 year after intervention (M12, with a score ≥2) were compared to those at baseline (M0, see also Supp. Figure 4). Data complexity was reduced by building a self-organizing map using a squared Euclidian distance metrics with 1,500 iterations allowing 10 gene clusters to be defined. These clusters are shown and those containing significantly dysregulated genes (paired t-test, FC>1.2, p<0.05; clusters 1-2 and 9-10) were annotated by GO term enrichment analysis (Figure 7) and selected for further analysis. Gene symbols are indicated below each cluster diagram which was generated by Genespring GX14.3.

Supplemental Table 6 – Identification of bariatric surgery-sensitive genes. Genes whose expression is significantly dysregulated (FC>1.2, p<0.05) in lobular inflammation or in ballooning or in fibrosis were extracted from microarray data as well as genes whose expression is significantly altered after bariatric surgery ("Condition-specific" worksheet). Gene lists were pooled ("Pooled" worksheet) to generate a list of

up- or down-regulated genes in advanced NASH (See also Figure 8A). Similarly, genes up- or down-regulated after bariatric surgery were pooled. These gene lists were compared in a pair-wise manner to identify genes up-regulated in severe NASH conditions, and down-regulated after bariatric surgery or down-regulated in severe NASH conditions, and up-regulated after bariatric surgery ("Overlap" worksheet).

Supplemental Table 7 – Differentially expressed genes in 3 independent cohorts. Microarray datasets from Arendt et al. and Moylan et al. were processed similarly to our dataset. Differentially expressed genes between control patients vs NASH/fibrotic patients (Arendt et al.) or mildly fibrotic vs advanced fibrotic patients (Moylan et al.) were identified (FC>1.2, $p<0.05$). Gene symbols and FC values are indicated. The gene signature for human advanced NASH was generated by comparing these 6 datasets and identifying genes common to up- or down-regulated gene lists.

Supplemental Table 8 – Modulated liver genes in MCD- and HF diet fed mice. Microarray data were analyzed to identify genes which were either significantly up- or down-regulated (unpaired t-test, FC>1.2, $p<0.05$).

Supplemental Table 9 – Modulated liver genes in HFD/CCl_4-treated mice. Microarray data were analyzed to identify genes which were either significantly up- or down-regulated after combined HFD-CCl_4 treatment (unpaired t-test, FC>1.2, $p<0.05$).

Supplemental Table 10 – Defining an inter-species core signature for definite NASH. Gene lists which were used to establish the core signature for advanced NASH are compiled in this table. See also Figure 4a.

Supplemental table 11 – Gene expression variation in CCl_4-treated mouse liver. Gene expression fold changes (FC>2) are provided together with p values.

Supplemental Table 12. Liver fibrosis modulator expression in human and mouse livers. Normalized expression values for the indicated genes involved in the fibrotic process were extracted from microarray data and are expressed as fold change (n=3-6, $p<0.05$). HSC: hepatic stellate cells, LSEC: liver sinusoidal endothelial cells, KC: Kuppfer cells; Hep: hepatocytes; WAT: white adipose tissue (visceral or peri-gonadal). Red: up-regulated genes, blue: down-regulated genes.

Supplemental Table 13 – *Dpt* gene inactivation affect the CCl_4-induced liver transcriptional response. Liver genes significantly dysregulated in CCl_4-treated $Dpt^{+/+}$ mice (see supplemental table 11) or in CCl_4-treated $Dpt^{-/-}$ mice were identified by an unpaired t-test (FC>2, $p<0.05$). Their relative regulation in the $Dpt^{+/+}$ or $Dpt^{-/-}$ background is expressed as the ratio of their FC upon CCl_4 treatment. A significance threshold of 2 (hence a ratio >2 or <0.5) was applied to select genes whose expression is markedly different in the $Dpt^{-/-}$ background. A scatter plot representation of these data can be found in figure 5A.

BIBLIOGRAPHY

1. Lukaski HC, Johnson PE, Bolonchuk WW, and Lykken GI. Assessment of fat-free mass using bioelectrical impedance measurements of the human body. *Am J Clin Nutr.* 1985;41(4):810-7.
2. Deurenberg P, Weststrate JA, and Hautvast JG. Changes in fat-free mass during weight loss measured by bioelectrical impedance and by densitometry. *Am J Clin Nutr.* 1989;49(1):33-6.
3. van der Kooy K, and Seidell JC. Techniques for the measurement of visceral fat: a practical guide. *Int J Obes Relat Metab Disord.* 1993;17(4):187-96.
4. Friedewald WT, Levy RI, and Fredrickson DS. Estimation of the concentration of low-density lipoprotein cholesterol in plasma, without use of the preparative ultracentrifuge. *Clin Chem.* 1972;18(6):499-502.
5. Matthews DR, Hosker JP, Rudenski AS, Naylor BA, Treacher DF, and Turner RC. Homeostasis model assessment: insulin resistance and beta-cell function from fasting plasma glucose and insulin concentrations in man. *Diabetologia.* 1985;28(7):412-9.
6. American Diabetes A. (2) Classification and diagnosis of diabetes. *Diabetes Care.* 2015;38 Suppl:S8-S16.
7. Alberti KG, Eckel RH, Grundy SM, Zimmet PZ, Cleeman JI, Donato KA, et al. Harmonizing the metabolic syndrome: a joint interim statement of the International Diabetes Federation Task Force on Epidemiology and Prevention; National Heart, Lung, and Blood Institute; American Heart Association; World Heart Federation; International Atherosclerosis Society; and International Association for the Study of Obesity. *Circulation.* 2009;120(16):1640-5.
8. Taylor KJ, Sullivan D, Simeone J, and Rosenfield AT. Scintigraphy, ultrasound and CT scanning of the liver. *Yale J Biol Med.* 1977;50(5):437-55.
9. Merkel C, Bolognesi M, Bellon S, Bianco S, Honisch B, Lampe H, et al. Aminopyrine breath test in the prognostic evaluation of patients with cirrhosis. *Gut.* 1992;33(6):836-42.
10. Younossi ZM, Jarrar M, Nugent C, Randhawa M, Afendy M, Stepanova M, et al. A novel diagnostic biomarker panel for obesity-related nonalcoholic steatohepatitis (NASH). *Obes Surg.* 2008;18(11):1430-7.
11. Verrijken A, Beckers S, Francque S, Hilden H, Caron S, Zegers D, et al. A gene variant of PNPLA3, but not of APOC3, is associated with histological parameters of NAFLD in an obese population. *Obesity (Silver Spring).* 2013;21(10):2138-45.

A

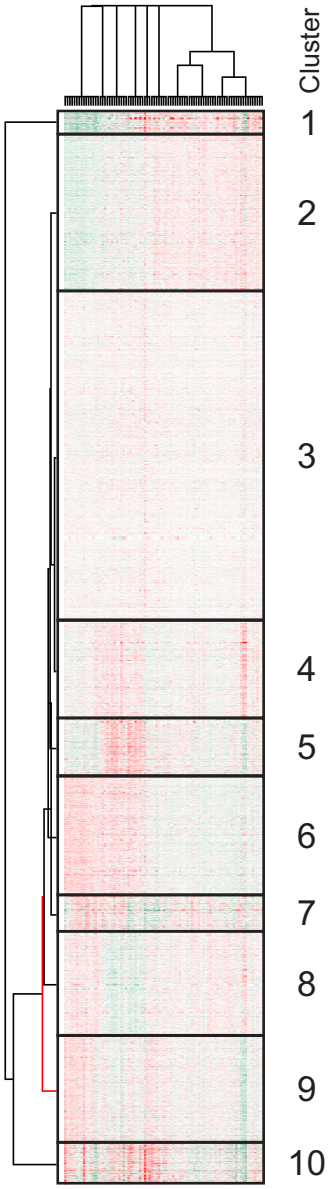

B

Cluster	Database	Term	Gene count	%	p value	Corrected p value (BH)
Cluster 1	OMIM_DISEASE	Common variants at 30 loci contribute to polygenic dyslipidemia	3	0,3	5,10E-02	9,80E-01
	SP_PIR_KEYWORDS	extracellular matrix	12	1,1	8,40E-08	2,30E-05
	GOTERM_BP_FAT	fatty acid biosynthetic process	5	0,4	2,40E-03	7,70E-01
	GOTERM_CC_FAT	extracellular matrix part	9	0,8	2,40E-06	5,10E-04
	GOTERM_MF_FAT	cytokine binding	5	0,4	4,80E-03	7,60E-01
	BIOCARTA	-	-	-	-	-
	KEGG_PATHWAY	Focal adhesion	6	0,5	4,30E-02	7,00E-01
Cluster 2	OMIM_DISEASE	Diabetes mellitus, noninsulin-dependent	6	0,1	1,00E-03	3,80E-01
	SP_PIR_KEYWORDS	extracellular matrix	41	0,4	1,10E-13	2,00E-11
	GOTERM_BP_FAT	Wnt receptor signaling pathway	27	0,2	9,90E-09	1,60E-05
	GOTERM_CC_FAT	proteinaceous extracellular matrix	55	0,5	2,80E-15	1,30E-12
	GOTERM_MF_FAT	extracellular matrix structural constituent	21	0,2	1,80E-08	1,70E-05
	BIOCARTA	Integrin Signaling Pathway	10	0,1	9,80E-03	9,00E-01
	KEGG_PATHWAY	Insulin signaling pathway	31	0,3	2,70E-07	2,10E-05
Cluster 3	OMIM_DISEASE	Epidermolysis bullosa, junctional, non-Herlitz type	3	0,2	8,10E-02	1,00E+00
	SP_PIR_KEYWORDS	Secreted	332	18,1	4,70E-41	8,70E-39
	GOTERM_BP_FAT	response to wounding	136	7,4	5,60E-19	1,20E-15
	GOTERM_CC_FAT	extracellular region part	261	14,2	1,40E-44	8,40E-42
	GOTERM_MF_FAT	cytokine activity	64	3,5	1,80E-14	2,50E-11
Cluster 4	OMIM_DISEASE	Newly identified loci that influence lipid concentrations and risk of coronary artery disease	5	1	1,30E-02	9,60E-01
	SP_PIR_KEYWORDS	mitochondrion	60	11,8	4,40E-12	2,20E-09
	GOTERM_BP_FAT	regulation of transcription from RNA polymerase II promoter	59	11,6	2,30E-10	5,80E-07
	GOTERM_CC_FAT	mitochondrion	69	13,5	5,20E-09	2,10E-06
	GOTERM_MF_FAT	transcription factor activity	66	12,9	3,40E-08	2,60E-05
	BIOCARTA	IL-2 Receptor Beta Chain in T cell Activation	5	1	6,70E-02	1,00E+00
Cluster 5	OMIM_DISEASE	Newly identified loci that influence lipid concentrations and risk of coronary artery disease	6	1,9	4,30E-04	6,80E-02
	SP_PIR_KEYWORDS	endoplasmic reticulum	34	10,9	5,70E-08	2,30E-05
	GOTERM_BP_FAT	sterol metabolic process	12	3,9	5,50E-06	1,10E-02
	GOTERM_CC_FAT	mitochondrion	47	15,1	3,80E-06	1,30E-03
	GOTERM_MF_FAT	identical protein binding	28	9	2,40E-04	1,40E-01
	BIOCARTA	Mechanism of Gene Regulation by Peroxisome Proliferators via PPARa(alpha)	7	2,3	7,80E-03	4,60E-01
	KEGG_PATHWAY	Citrate cycle (TCA cycle)	6	1,9	3,10E-03	3,70E-01
Cluster 6	OMIM_DISEASE	Framingham Heart Study 100K Project	4	0,6	2,70E-02	1,00E+00
	SP_PIR_KEYWORDS	acetylation	205	31,5	1,20E-32	6,60E-30
	GOTERM_BP_FAT	RNA elongation from RNA polymerase II promoter	15	2,3	6,20E-09	1,70E-05
	GOTERM_CC_FAT	membrane-enclosed lumen	146	22,5	2,10E-17	9,20E-15
	GOTERM_MF_FAT	threonine-type endopeptidase activity	8	1,2	1,10E-05	8,80E-03
	BIOCARTA	FAS signaling pathway (CD95)	7	1,1	2,40E-02	9,90E-01
	KEGG_PATHWAY	Proteasome	14	2,2	1,60E-06	2,60E-04
Cluster 7	OMIM_DISEASE	Association of three genetic loci with uric acid concentration and risk of gout	2	1	5,80E-02	1,00E+00
	SP_PIR_KEYWORDS	oxidoreductase	35	17,9	2,70E-17	9,30E-01
	GOTERM_BP_FAT	oxidation reduction	35	17,9	3,90E-13	6,10E-10
	GOTERM_CC_FAT	mitochondrion	36	18,4	2,20E-08	4,90E-06
	GOTERM_MF_FAT	electron carrier activity	19	9,7	4,30E-10	2,20E-07
	BIOCARTA	Nuclear Receptors in Lipid Metabolism and Toxicity	6	3,1	7,90E-04	6,80E-02
	KEGG_PATHWAY	Valine, leucine and isoleucine degradation	12	6,1	3,50E-09	4,60E-07
Cluster 8	OMIM_DISEASE	Robust associations of four chromosome regions from genome-wide analyses of type 1 diabetes	3	1	3,60E-02	1,00E+00
	SP_PIR_KEYWORDS	phosphoprotein	194	63,8	3,90E-21	1,30E-18
	GOTERM_BP_FAT	death	31	10,2	1,90E-05	3,60E-02
	GOTERM_CC_FAT	cytosol	49	16,1	4,60E-07	1,50E-04
	GOTERM_MF_FAT	nucleoside binding	64	21,1	5,80E-08	3,30E-05
	BIOCARTA	MAPKinase Signaling Pathway	9	3	1,30E-02	8,40E-01
	KEGG_PATHWAY	Ubiquitin mediated proteolysis	15	4,9	2,90E-05	3,90E-03
Cluster 9	OMIM_DISEASE	Variants in TF and HFE explain approximately 40% of genetic variation in serum-transferrin levels	3	1,3	4,20E-02	1,00E+00
	SP_PIR_KEYWORDS	phosphoprotein	148	62,7	8,90E-15	2,80E-12
	GOTERM_BP_FAT	protein kinase cascade	23	9,7	9,10E-08	1,50E-04
	GOTERM_CC_FAT	nuclear lumen	48	20,3	2,50E-08	7,30E-06
	GOTERM_MF_FAT	protein kinase activity	26	11	1,10E-05	5,70E-03
	BIOCARTA	Nuclear receptors coordinate the activities of chromatin remodeling complexes	3	1,3	8,10E-02	1,00E+00
	KEGG_PATHWAY	RNA degradation	7	3	1,00E-03	1,20E-01
Cluster 10	OMIM_DISEASE	Multiple sclerosis, susceptibility to	3	1,3	7,50E-03	7,40E-01
	SP_PIR_KEYWORDS	signal	119	53,1	4,10E-35	1,50E-32
	GOTERM_BP_FAT	immune response	50	22,3	1,60E-21	3,20E-18
	GOTERM_CC_FAT	extracellular region part	59	26,3	3,30E-19	7,70E-17
	GOTERM_MF_FAT	extracellular matrix structural constituent	9	4	2,00E-05	4,50E-03
	BIOCARTA	Pertussis toxin-insensitive CCR5 Signaling in Macrophage	4	1,8	9,80E-03	6,60E-01
	KEGG_PATHWAY	Cell adhesion molecules (CAMs)	13	5,8	3,30E-05	3,80E-03

Supplemental Figure 1

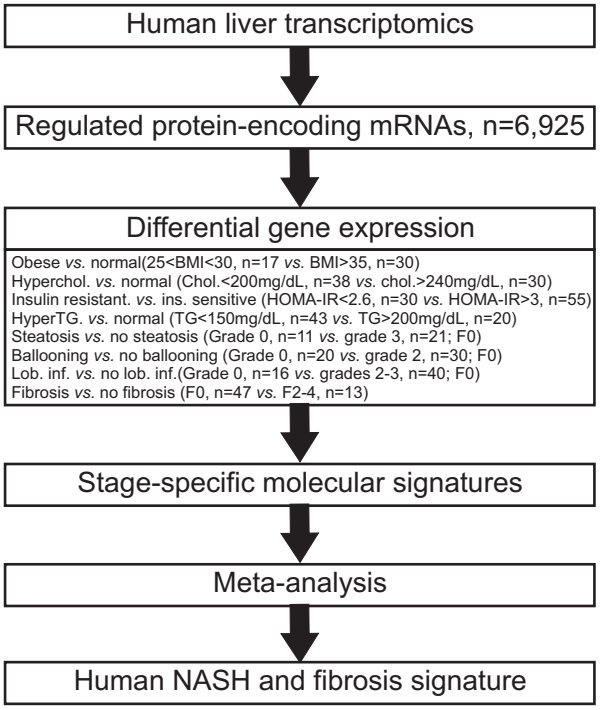

Supplemental Figure 2

A- Gene expression in fibrosis

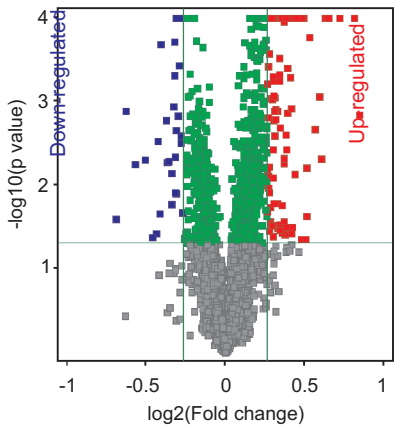

B- Biological processes in fibrosis

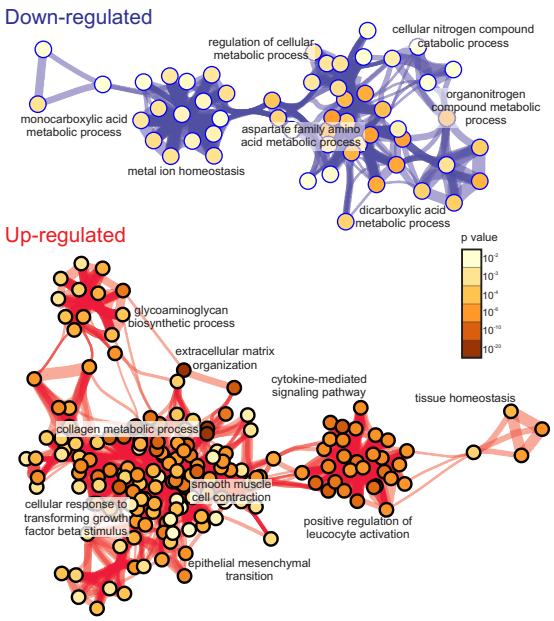

Supplemental Figure 3

A-Up-regulated genes by GABY

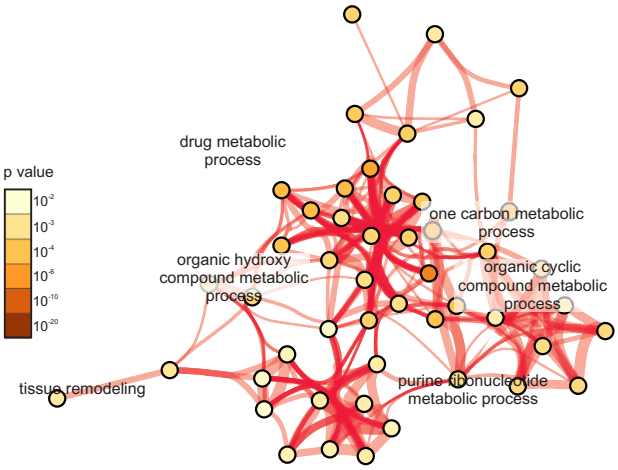

B-Down-regulated genes by GABY

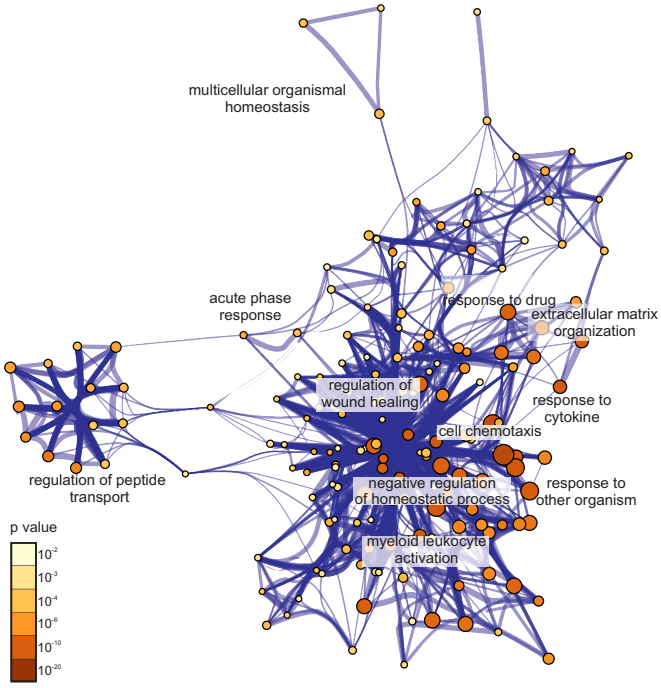

Supplemental Figure 4

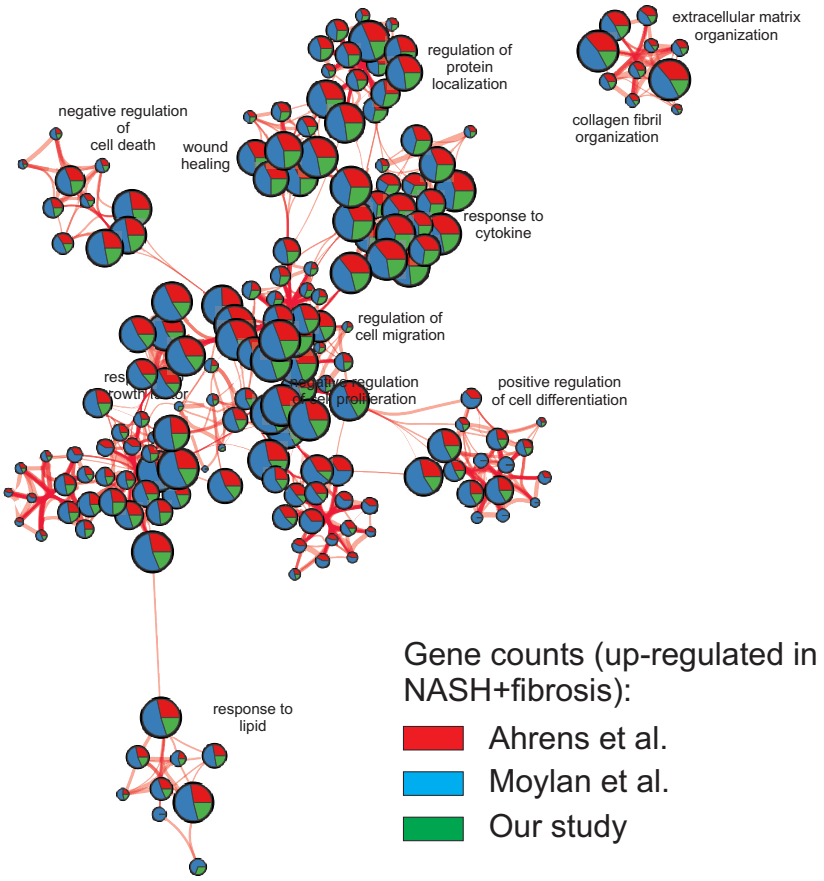

Supplemental Figure 5

A-Genes up-regulated in human NASH+fibrosis

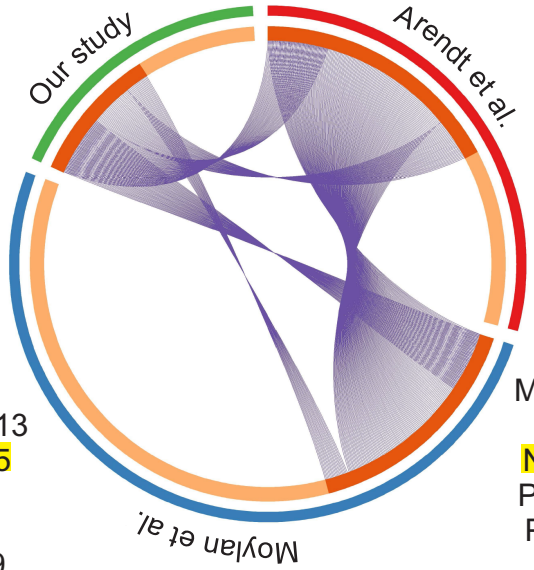

ACLY				MARCKS
ANXA13				MMP2
ANXA5				NUSAP1
ASPN				PDGFRA
C7				PRKAA2
CCL19				PTGDS
CCL21				PTGIS
CCND1				SCPEP1
CD24				SNAP25
CHI3L1	CXCL10	FAT1	ITGAV	SPP1
CLDN10	CXCL9	FBLN5	JAG1	SULF2
COL14A1	DPT	FMOD	KPNA2	THBS2
COL1A1	DTNA	GUCY1A3	LAMA2	TIMP1
COL1A2	EFEMP1	IGFBP7	LUM	UBD
COL3A1	FABP4	IL32	LYZ	ZMAT3

B-Genes down-regulated in human NASH+fibrosis

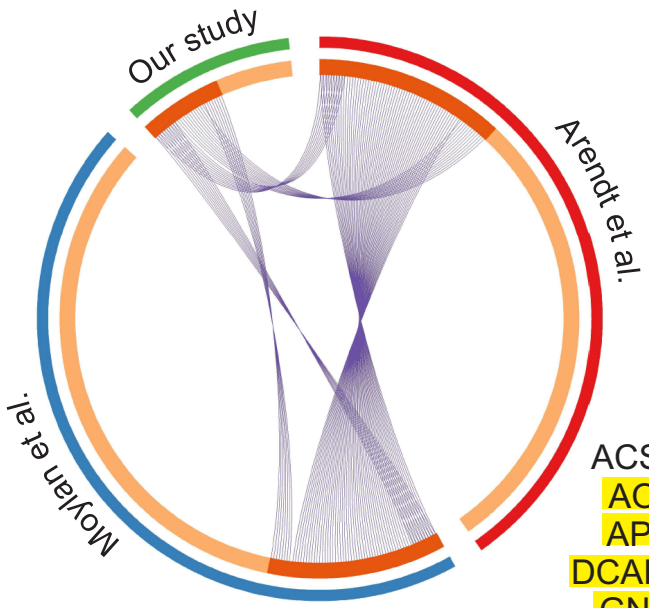

ACSL5
AOX1
APOF
DCAF11
GNMT
KCNMA1
KCNN2
N4BP2L1
ST3GAL1
TTC36

: normalized by BarSur

Supplemental Figure 6

A - Genes up-regulated in HF/MCD diet-fed mouse livers

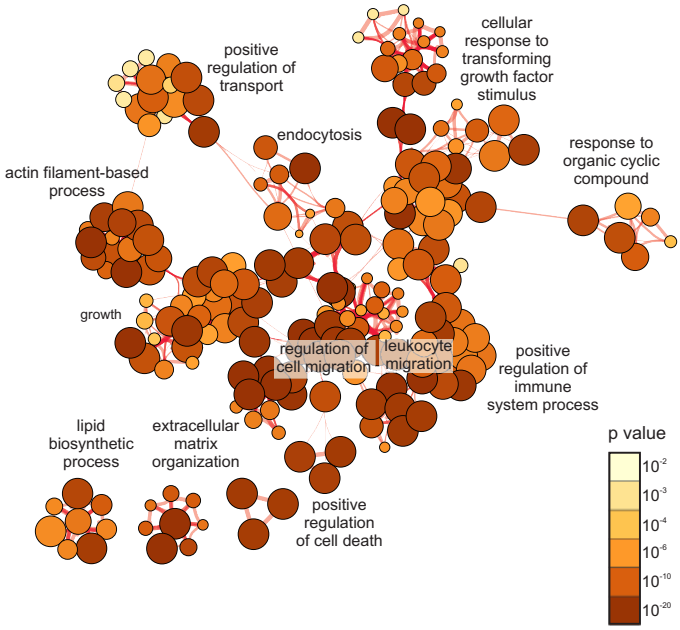

B - Genes down-regulated in HF/MCD diet-fed mouse livers

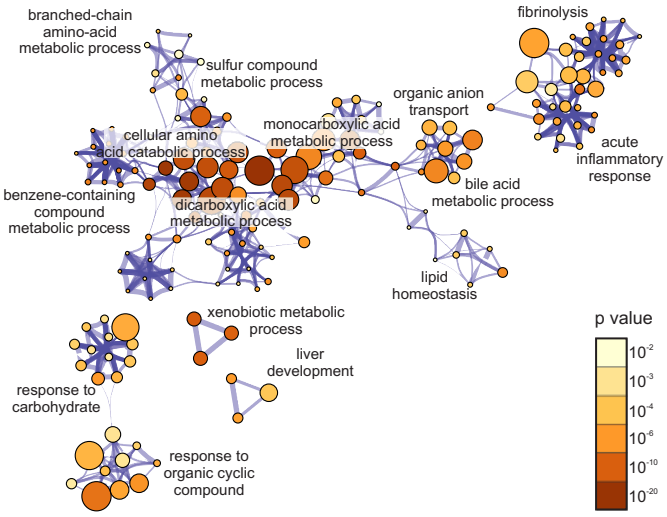

Supplemental Figure 7

A - Genes up-regulated in
CCl_4-treated, HFdiet-fed mouse livers

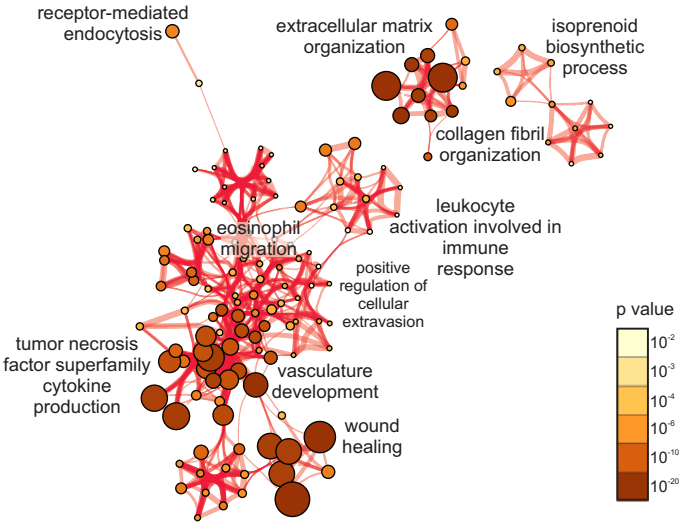

B - Genes down-regulated in
CCl_4-treated, HFdiet-fed mouse livers

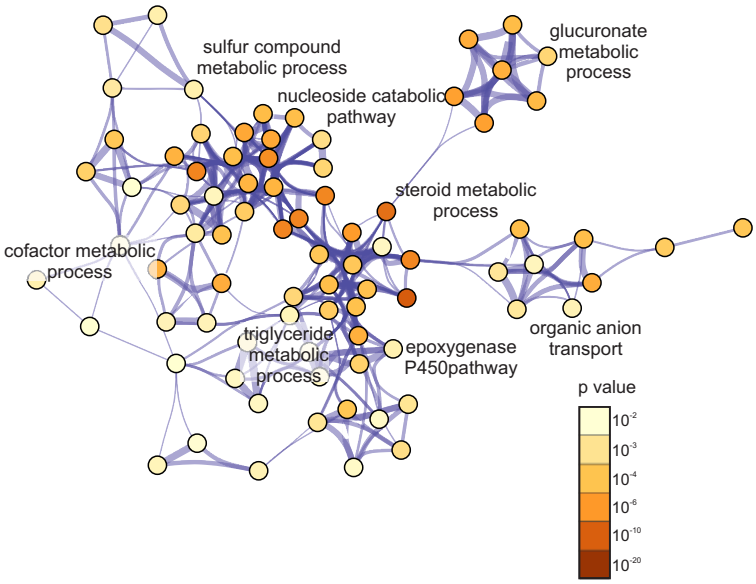

Supplemental Figure 8

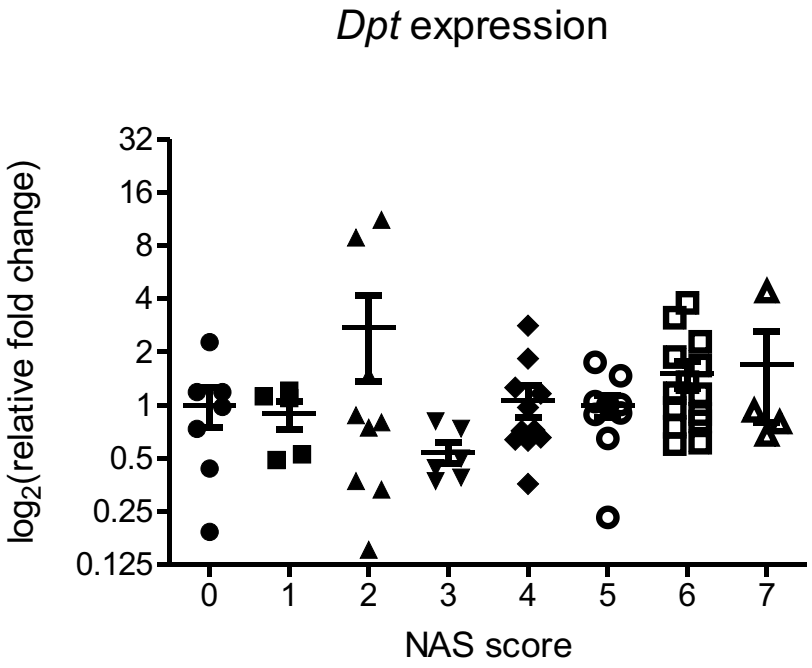

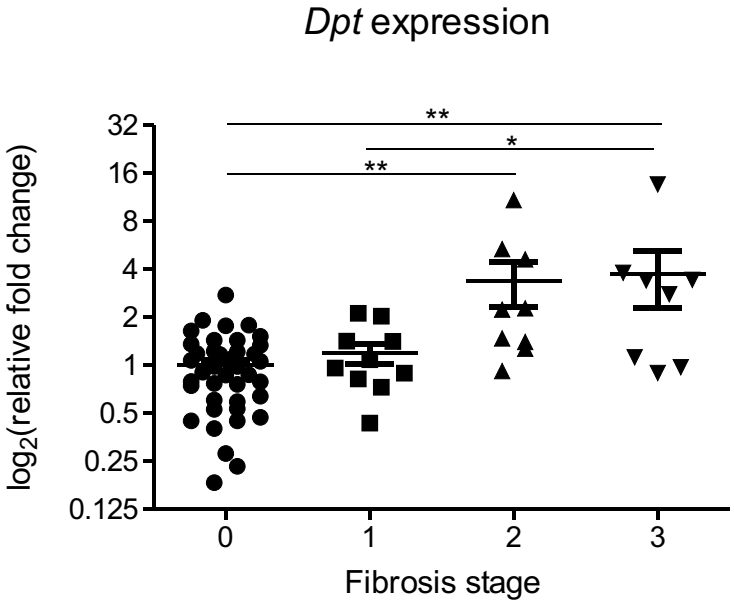

Supplemental Figure 9

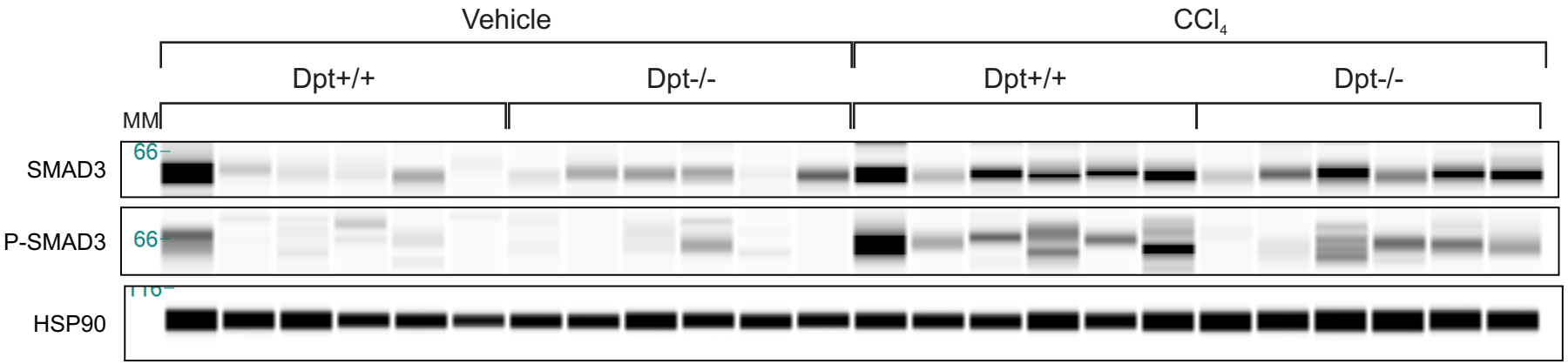

Supplemental Figure 10

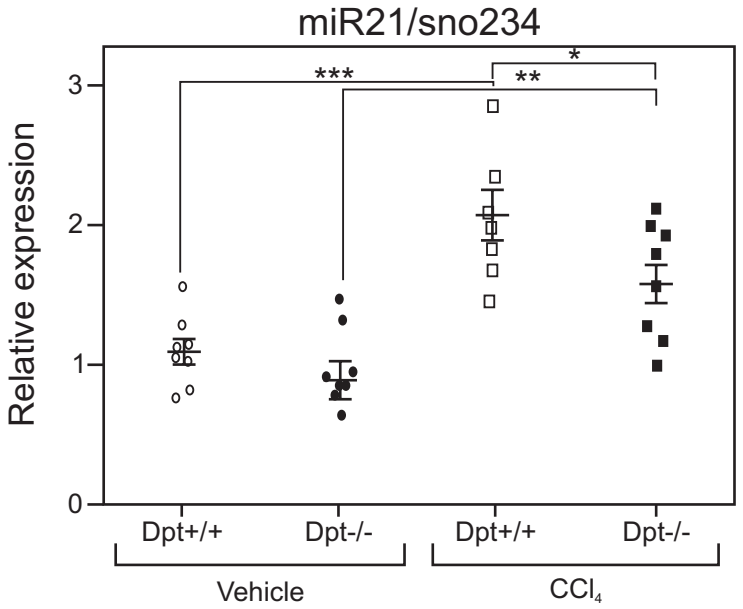

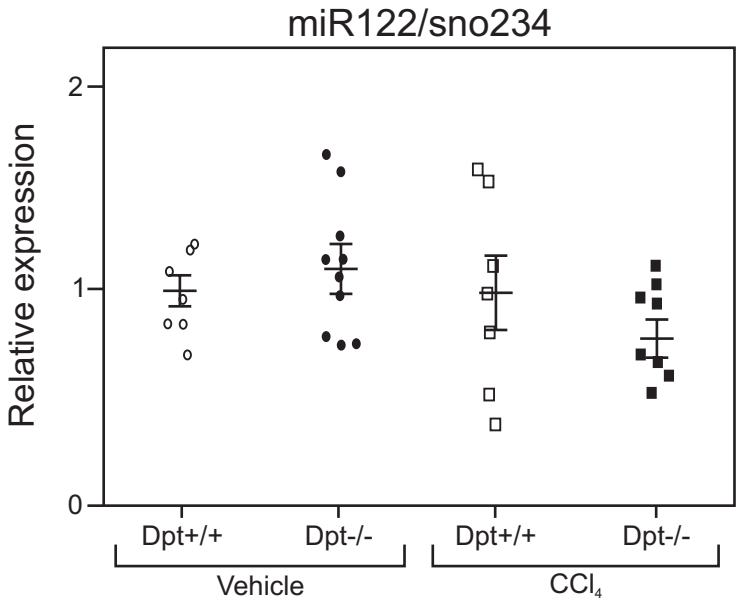

Supplemental Figure 11

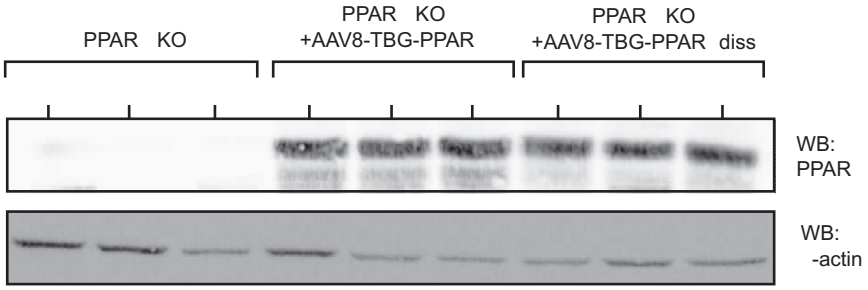

Supplemental Figure 12